Wind and Structures, *Vol. 32, No. 1 (2021) 19-30*
DOI: https://doi.org/10.12989/was.2021.32.1.19

Buckling analysis of sandwich plates with functionally graded porous layers using hyperbolic shear displacement model

Lazreg Hadji*[1,2]

[1]*Laboratory of Geomatics and Sustainable Development, University of Tiaret, Algeria*
[2]*Department of Mechanical Engineering, University of Tiaret, BP 78 Zaaroura, Tiaret,14000, Algeria*

(*Received May 14, 2020, Revised December 13, 2020, Accepted December 14, 2020*)

Abstract. This study presents buckling analysis of a simply supported sandwich plate with functionally graded porous layers. In the kinematic relation of the plate, a hyperbolic shear displacement model is used. The governing equations of the problem are derived by using the principle of virtual work. In the solution of the governing equations, the Navier procedure is implemented. In the porosity effect, four different porosity types are used for functionally graded sandwich layers. In the numerical examples, the effects of the porosity parameters, porosity types and geometry parameters on the critical buckling of the functionally graded sandwich plates are investigated.

Keywords: buckling; sandwich plates; functionally graded materials; porosity; higher-order plate theory

1. Introduction

Functionally graded materials (FGM) are a new generation of a composite material whose properties change gradually along a direction. Since 1984, the using and investigations of functionally graded materials have been increasing. Functionally graded materials have many advantages in contrast with classical composites.

Porosities could occur due to production or technical errors in the functionally graded materials. This is because of the large difference in solidification temperatures between material constituents (Zhu *et al.* 2001). With porosity, the mechanical behavior of functionally graded materials changes considerably. Thus, the effect of the porosity on the functionally graded materials is an important problem and must be investigated in order to safe design of this composites.

In last years, many researchers interested in investigation of porous functionally graded materials; Wattanasakulpong and Ungbhakorn (2014) studied vibration characteristics of FGM porous beams by using differential transformation method with different kinds of elastic supports. Ebrahimi and Jafari (2016) investigated thermal vibration of FGM porous beams. Hadji *et al.* (2016) studied effects of porosity on the static and vibration responses of FGM beams by using Navier solution. Wu *et al.* (2018) performed a finite element analysis to study the free and forced vibration FGM porous beam using both Euler-Bernoulli and Timoshenko beam theories.Yang *et al* . (2018) used Chebyshev-Ritz method to study buckling and free vibration of FGM graphene reinforced porous nanocomposite. Akbaş (2017) examined the vibration and static analysis of functionally graded plates with porosity. Fazzolari (2018) exploited generalized beam theories to study the vibration and stability of porous FGM sandwich beams resting on elastic foundations. Jouneghani *et al.* (2018) studied analytically the structural response of porous FGM nonlocal nanobeams under hygro-thermo-mechanical loadings. Bennai *et al.* (2019) investigated the dynamic and wave propagation of FGM plates with porosities using a four variable plate theory. Avcar (2019) examined the free vibration of functionally graded beams with porosity with different porosity distribution models. Ramteke *et al.* (2019) studied effects of the porosity on the Eigen characteristics of functionally graded structures with different types of porosity and material distributions. Benahmed (2019) investigated buckling analysis of FGM nanobeams with porosity by using higher-order shear deformation theory. Taati and Fallah (2019) presented forced vibration of sandwich modified strain gradient microbeams with FGM core. Xu *et al.* (2019) studied buckling analysis of functionally graded porous plates with laminated face sheets by using finite element method based on first order shear deformation theory. Zhao *et al.* (2019) investigated vibration behavior of the FGM porous curved thick beam, doubly-curved panels and shells of revolution by using a semi-analytical method. Keddouri *et al.* (2019) presented static responses of functionally graded plates with porosity effects by using the Navier method. Alimirzaei *et al.* (2019) studied nonlinear analysis of viscoelastic micro-composite beam with geometrical imperfection using FEM: MSGT electro-magneto-elastic bending, buckling and vibration solutions. Addou *et al.* (2019) investigated the influences of porosity on dynamic response of FG plates resting on Winkler/Pasternak/Kerr foundation using quasi 3D HSDT. Medani *et al.* (2019) developed static and dynamic behavior of (FG-CNT) reinforced porous sandwich plate using energy principle. Alimirzaei *et al.* (2019) studied nonlinear analysis of viscoelastic micro-composite beam

*Corresponding author, Ph.D.
E-mail: had_laz@yahoo.fr

http://www.techno-press.com/journals/was&subpage=7
ISSN: 1226-6116 (Print), 1598-6225 (Online)

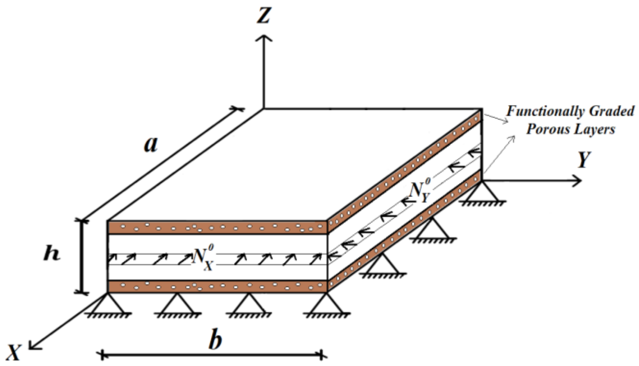

Fig. 1 Geometry of a simply supported sandwich rectangular plate with functionally graded porous layers

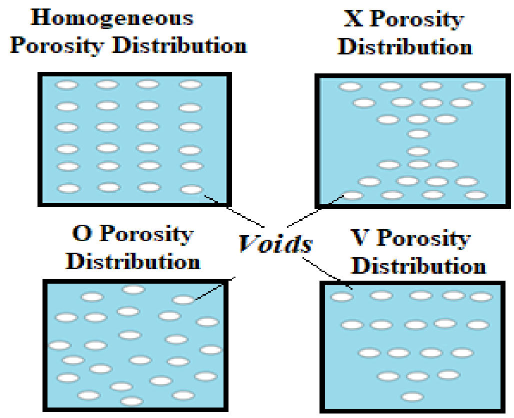

Fig. 2 Porosity Distribution Models

with geometrical imperfection using FEM: MSGT electro-magneto-elastic bending, buckling and vibration solutions. Berghouti *et al.* (2019), "Vibration analysis of nonlocal porous nanobeams made of functionally graded material. Bourada *et al.* (2019), studied dynamic investigation of porous functionally graded beam using a sinusoidal shear deformation theory. Batou *et al.* (2019), developed wave dispersion properties in imperfect sigmoid plates using various HSDTs. Kaddari *et al.* (2020) used a new quasi-3D model for structural behaviour of functionally graded porous plates on elastic foundation. Hadji and Avcar (2021) studied the free vibration analysis of FG porous sandwich plates under various boundary conditions.

Since shear deformation theories are widely used in FGM structures, the first-order shear deformation theory and higher-order shear deformation theories should be used. By using these theories, many papers have been developed to study static, vibration and buckling analysis of FG and nano structures such as (Karami *et al.* 2019, Boutaleb *et al.* 2019, Safa *et al.* 2019, Balubaid *et al.* 2019, Hussain *et al.* 2019, Belbachir *et al.* 2019, Sahla *et al.* 2019, Abualnour *et al.* 2019, Draiche *et al.* 2019, Tounsi *et al.* 2020, Refrafi *et al.* 2020, Chikr, *et al.* 2020, Matouk *et al.* 2020, Rahmani *et al.* 2020, Bousahla *et al.* 2020a, 2020b, Bellal *et al.* 2020, Belbachir *et al.* 2020, Shariati *et al* . 2020a, 2020b; Bourada *et al.* 2020, Hussain *et al.* 2020a, 2020b, Asghar *et al.* 2020, Taj *et al.* 2020).

Recently, many researchs focus on the study of buckling of FG structures; Zenkour and Sobhy (2010) investigated the thermal buckling of various types of FGM sandwich plates. Trinh *et al.* (2018), used state-space levy solution for size-dependent static, free vibration and buckling behaviours of functionally graded sandwich plates. Karamanli and Aydogdu (2020) studied the bifurcation buckling conditions of FGM plates with different boundaries.

In this study, buckling analysis of a simply supported sandwich plate with functionally graded layers whose properties are porous. The buckling problem is solved by using the Navier method based on the higher-order shear deformation plate theory. In the numerical examples, the effects of the porosity parameters and porosity types in FGM layers, geometry parameters on the critical buckling of the functionally graded sandwich plates are presented and discussed. The contribution of this study on literature is to present and investigate the effects of porosity on the buckling behavior of FGM sandwich plates.

2. Problem formulation

A simply supported sandwich rectangular plate with porous functionally graded face layers subjected to biaxial compressive loads in X and Y directions is shown in Fig. 1. Where, a, b and h indicate the dimension in the X, Y and Z directions, respectively.

The sandwich plate is made of three layers, an isotropic core and two power-law functionally gradedlayers. The material properties of the face layers vary from metal to ceramic and the core layer is made of ceramic. The volume fraction $^{(n)}$ of layer n (n=1,2,3), varies according to the following power-law function across the plate thickness

$$V^{(1)}(Z)=\left(\frac{Z-h_1}{h_2-h_1}\right)^n \quad h_1\leq Z\leq h_2 \tag{1a}$$

$$V^{(2)}(Z)=1 \quad h_2\leq Z\leq h_3 \tag{1b}$$

$$V^{(3)}(Z)=\left(\frac{Z-h_4}{h_3-h_4}\right)^n \quad h_3\leq Z\leq h_4 \tag{1c}$$

where h_1, h_2 and h_3 are the bottom surface coordinates of the bottom face layer, the core layer and the top layer respectively. Likewise, h_2, h_3 and h are the top surface coordinates of the bottom face layer, the core layer and the top layer respectively. In equation 1, n indicates the power-law coefficient (volume fraction index). When n=0, the material of plate gets homogenous ceramic.

In the porosity distribution of functionally graded layers, four different porosity distribution models are used. These porosity distribution models are shown in Fig. 2. Used the porosity models in this study are; homogeneous porosity distribution, X porosity distribution, O porosity distribution and V porosity distribution.

According to these models, the effective material properties (P) for each layers are given as follows:

For Homogeneous Porosity Distribution:

$$\begin{cases} P^{(1)}(z) = P_m + (P_c - P_m)V^{(1)}(z) - \frac{\xi}{2}(P_c + P_m) \\ P^{(2)}(z) = P_m + (P_c - P_m)V^{(2)}(z) \\ P^{(3)}(z) = P_m + (P_c - P_m)V^{(3)}(z) - \frac{\xi}{2}(P_c + P_m) \end{cases} \quad (2)$$

For X Porosity Distribution:

$$\begin{gathered} P^{(1)}(z) = P_m + (P_c - P_m)V^{(1)}(z) - \frac{\xi}{2}(P_c + P_m)\left|\frac{2z-(h_1+h_2)}{h_1-h_2}\right| \\ P^{(2)}(z) = P_m + (P_c - P_m)V^{(2)}(z) \\ P^{(3)}(z) = P_m + (P_c - P_m)V^{(3)}(z) - \frac{\xi}{2}(P_c + P_m)\left|\frac{2z-(h_3+h_4)}{h_3-h_4}\right| \end{gathered} \quad (3)$$

For O Porosity Distribution:

$$\begin{cases} P^{(1)}(z) = P_m + (P_c - P_m)V^{(1)}(z) - \frac{\xi}{2}(P_c + P_m)\sqrt{\left(\frac{h_1-h_2}{2}\right)^2 - \left(z - \left(\frac{h_1+h_2}{2}\right)\right)^2} \\ P^{(2)}(z) = P_m + (P_c - P_m)V^{(2)}(z) \\ P^{(3)}(z) = P_m + (P_c - P_m)V^{(3)}(z) - \frac{\xi}{2}(P_c + P_m)\sqrt{\left(\frac{h_3-h_4}{2}\right)^2 - \left(z - \left(\frac{h_3+h_4}{2}\right)\right)^2} \end{cases} \quad (4)$$

For V Porosity Distribution:

$$\begin{cases} P^{(1)}(z) = P_m + (P_c - P_m)V^{(1)}(z) - \frac{\xi}{2}(P_c + P_m)\left(\frac{z-h_2}{h_1-h_2}\right) \\ P^{(2)}(z) = P_m + (P_c - P_m)V^{(2)}(z) \\ P^{(3)}(z) = P_m + (P_c - P_m)V^{(3)}(z) - \frac{\xi}{2}(P_c + P_m)\left(\frac{z-h_4}{h_3-h_4}\right) \end{cases} \quad (5)$$

where ξ $(\xi < 1)$ demotes the the volume fraction of porosity.

Based on the higher-order shear deformation plate theory, the displacement fields of the plate are presented as follows:

$$\begin{aligned} u(x,y,z,t) &= u_0(x,y,t) - z\frac{\partial w_0}{\partial x} + k_1\, f(z)\int \theta(x,y,t)\,dx \\ v(x,y,z,t) &= v_0(x,y,t) - z\frac{\partial w_0}{\partial y} + k_2\, f(z)\int \theta(x,y,t)\,dy \\ w(x,y,z,t) &= w_0(x,y,t) \end{aligned} \quad (6)$$

Where, *u*, *v* and *w* are the displacements functions of *X*, *Y* and *Z* directions, respectively. u_0, v_0 and w_0 and θ are the four unknown displacement of the mid-plane of the plate. In equation (6), *f*(z) is defined according to the higher-order shear deformation plate as follows:

$$f(z) = \frac{3}{2}\pi h \tanh\left(\frac{z}{h}\right) - \frac{3}{2}\pi z \sec h\left(\frac{1}{2}\right)^2 \quad (7)$$

It can be seen that the displacement field in Eq. (6) introduces only four unknowns (u_0, v_0, w_0 and θ). The nonzero strains associated with the displacement field in Eq. (6) are

$$\begin{Bmatrix} \varepsilon_x \\ \varepsilon_y \\ \gamma_{xy} \end{Bmatrix} = \begin{Bmatrix} \varepsilon_x^0 \\ \varepsilon_y^0 \\ \gamma_{xy}^0 \end{Bmatrix} + z\begin{Bmatrix} k_x^b \\ k_y^b \\ k_{xy}^b \end{Bmatrix} + f(z)\begin{Bmatrix} k_x^s \\ k_y^s \\ k_{xy}^s \end{Bmatrix} \quad (8a)$$

$$\begin{Bmatrix} \gamma_{yz} \\ \gamma_{xz} \end{Bmatrix} = g(z)\begin{Bmatrix} \gamma_{yz}^0 \\ \gamma_{xz}^0 \end{Bmatrix} \quad (8b)$$

Where

$$\begin{Bmatrix} \varepsilon_x^0 \\ \varepsilon_y^0 \\ \gamma_{xy}^0 \end{Bmatrix} = \begin{Bmatrix} \frac{\partial u_0}{\partial x} \\ \frac{\partial v_0}{\partial x} \\ \frac{\partial u_0}{\partial y} + \frac{\partial v_0}{\partial x} \end{Bmatrix}, \quad \begin{Bmatrix} k_x^b \\ k_y^b \\ k_{xy}^b \end{Bmatrix} = \begin{Bmatrix} -\frac{\partial^2 w_0}{\partial x^2} \\ -\frac{\partial^2 w_0}{\partial y^2} \\ -2\frac{\partial^2 w_0}{\partial x \partial y} \end{Bmatrix} \quad (9a)$$

$$\begin{Bmatrix} k_x^s \\ k_y^s \\ k_{xy}^s \end{Bmatrix} = \begin{Bmatrix} k_1\theta \\ k_2\theta \\ k_1\frac{\partial}{\partial y}\int \theta\,dx + k_2\frac{\partial}{\partial x}\int \theta\,dy \end{Bmatrix}, \quad \begin{Bmatrix} \gamma_{yz}^0 \\ \gamma_{xz}^0 \end{Bmatrix} = \begin{Bmatrix} k_2\int \theta\,dy \\ k_1\int \theta\,dx \end{Bmatrix} \quad (9b)$$

and

$$g(z) = \frac{df(z)}{dz} \quad (10)$$

The integrals defined in the above equations shall be resolved by a Navier type method and can be written as follows:

$$\begin{gathered} \frac{\partial}{\partial y}\int \theta\,dx = A'\frac{\partial^2\theta}{\partial x\partial y}, \quad \frac{\partial}{\partial x}\int \theta\,dy = B'\frac{\partial^2\theta}{\partial x\partial y} \\ \int \theta\,dx = A'\frac{\partial\theta}{\partial x}, \quad \int \theta\,dy = B'\frac{\partial\theta}{\partial y} \end{gathered} \quad (11)$$

where the coefficients A' and B' are expressed according to the type of solution used, in this case via Navier. Therefore, A', B', k_1 and k_2 are expressed as follows:

$$A' = -\frac{1}{\alpha^2}, \quad B' = -\frac{1}{\beta^2}, \quad k_1 = \alpha^2, \quad k_2 = \beta^2 \quad (12)$$

where α and β are defined in expression (28). For elastic and isotropic FGMs, the constitutive relations can be expressed as:

$$\begin{Bmatrix} \sigma_x \\ \sigma_y \\ \tau_{xy} \\ \tau_{yz} \\ \tau_{xz} \end{Bmatrix} = \begin{bmatrix} C_{11} & C_{12} & 0 & 0 & 0 \\ C_{12} & C_{22} & 0 & 0 & 0 \\ 0 & 0 & C_{66} & 0 & 0 \\ 0 & 0 & 0 & C_{44} & 0 \\ 0 & 0 & 0 & 0 & C_{55} \end{bmatrix} \begin{Bmatrix} \varepsilon_x \\ \varepsilon_y \\ \gamma_{xy} \\ \gamma_{yz} \\ \gamma_{xz} \end{Bmatrix} \quad (13)$$

where (σ_x, σ_y, τ_{xy}, τ_{yz}, τ_{xz}) and (ε_x, ε_y, γ_{xy}, γ_{yz}, γ_{xz}) are the stress and strain components, respectively. C_{ij} are the stiffness coefficients and can be given as

$$\begin{gathered} C_{11} = C_{22} = \frac{E(z)}{1-\nu^2}, \; C_{12} = \frac{\nu\, E(z)}{1-\nu^2}, \\ C_{44} = C_{55} = C_{66} = \frac{E(z)}{2(1+\nu)}, \end{gathered} \quad (14)$$

The governing equations of equilibrium can be derived by using the principle of virtual displacements. The principle of virtual work in the present case yields

$$\int_{-h/2}^{h/2}\int_{\Omega}\begin{bmatrix}\sigma_x\delta\varepsilon_x+\sigma_y\delta\varepsilon_y+\tau_{xy}\delta\gamma_{xy}\\+\tau_{xz}\delta\gamma_{xz}+\tau_{yz}\delta\gamma_{yz}\end{bmatrix}d\Omega dz.$$
$$+\int_{\Omega}\left(N_x^0\frac{\partial w_0}{\partial x}\frac{\partial\delta w_0}{\partial x}+N_y^0\frac{\partial w_0}{\partial y}\frac{\partial\delta w_0}{\partial y}+N_{xy}^0\frac{\partial w_0}{\partial x}\frac{\partial\delta w_0}{\partial y}\right)d\Omega=0 \tag{15}$$

where

$$\begin{Bmatrix}N_x, & N_y, & N_{xy}\\ M_x^b, & M_y^b, & M_{xy}^b\\ M_x^s, & M_y^s, & M_{xy}^s\end{Bmatrix}=\int_{-h/2}^{h/2}(\sigma_x,\sigma_y,\tau_{xy})\begin{Bmatrix}1\\ z\\ f(z)\end{Bmatrix}dz \tag{16a}$$

and

$$\left(S_{xz}^s,S_{yz}^s\right)=\int_{-h/2}^{h/2}(\tau_{xz},\tau_{yz})g(z)dz \tag{16b}$$

The governing equations of equilibrium can be derived from Eq. (15) by integrating the displacement gradients by parts and setting the coefficients zero δu_0, δv_0, δw_0, and $\delta\theta$ separately. Thus one can obtain the equilibrium equations associated with the present refined shear deformation plate theory

$$\delta u_0:\ \frac{\partial N_x}{\partial x}+\frac{\partial N_{xy}}{\partial y}=0$$
$$\delta v_0:\ \frac{\partial N_{xy}}{\partial x}+\frac{\partial N_y}{\partial y}=0$$
$$\delta w_0:\ \frac{\partial^2 M_x^b}{\partial x^2}+2\frac{\partial^2 M_{xy}^b}{\partial x\partial y}+\frac{\partial^2 M_y^b}{\partial y^2}+N_x^0\frac{\partial w_0}{\partial x}\frac{\partial\delta w_0}{\partial x}$$
$$+N_y^0\frac{\partial w_0}{\partial y}\frac{\partial\delta w_0}{\partial y}+N_{xy}^0\frac{\partial w_0}{\partial x}\frac{\partial\delta w_0}{\partial y}=0 \tag{17}$$
$$\delta\theta:\ -\mathrm{k}_1 M_x^s-\mathrm{k}_2 M_y^s-(k_1A'+k_2B')\frac{\partial^2 M_{xy}^s}{\partial x\partial y}$$
$$+k_1A'\frac{\partial S_{xz}^s}{\partial x}+k_2B'\frac{\partial S_{yz}^s}{\partial y}=0$$

Substituting Eq. (13) into Eq. (16) and integrating through the thickness of the plate, the stress resultants are given as

$$\begin{Bmatrix}N\\ M^b\\ M^s\end{Bmatrix}=\begin{bmatrix}A & B & B^s\\ B & D & D^s\\ B^s & D^s & H^s\end{bmatrix}\begin{Bmatrix}\varepsilon\\ k^b\\ k^s\end{Bmatrix},\ S=A^s\gamma \tag{18}$$

The stiffness coefficients A_{ij}, B_{ij} and D_{ij}, etc., are defined as

$$\begin{Bmatrix}A_{11} & B_{11} & D_{11} & B_{11}^s & D_{11}^s & H_{11}^s\\ A_{12} & B_{12} & D_{12} & B_{12}^s & D_{12}^s & H_{12}^s\\ A_{66} & B_{66} & D_{66} & B_{66}^s & D_{66}^s & H_{66}^s\end{Bmatrix}$$
$$=\int_{-h/2}^{h/2}C_{11}\left(1,z,z^2,f(z),z\ f(z),f^2(z)\right)\begin{Bmatrix}1\\ \nu\\ \frac{1-\nu}{2}\end{Bmatrix}dz \tag{19a}$$

$$\left(A_{22},B_{22},D_{22},B_{22}^s,D_{22}^s,H_{22}^s\right)=\left(A_{11},B_{11},D_{11},B_{11}^s,D_{11}^s,H_{11}^s\right) \tag{19b}$$

$$A_{44}^s=A_{55}^s=\int_{-h/2}^{h/2}C_{44}[g(z)]^2dz, \tag{19b}$$

$$A_{44}^s=A_{55}^s=\int_{-h/2}^{h/2}C_{44}[g(z)]^2dz, \tag{19c}$$

Introducing Eq. (18) into Eq. (17), the equations of motion can be expressed in terms of displacements (u_0, v_0, w_0, θ) and the appropriate equations take the form:

$$A_{11}d_{11}u_0+A_{66}d_{22}u_0+(A_{12}+A_{66})d_{12}v_0-B_{11}d_{111}w_0-(B_{12}+2B_{66})d_{122}w_0$$
$$+\left(B_{66}^s(k_1A'+k_2B')\right)d_{122}\theta+\left(B_{11}^sk_1+B_{12}^sk_2\right)d_1\theta=0, \tag{20a}$$

$$A_{22}d_{22}v_0+A_{66}d_{11}v_0+(A_{12}+A_{66})d_{12}u_0-B_{22}d_{222}w_0$$
$$-(B_{12}+2B_{66})d_{112}w_0+\left(B_{66}^s(k_1A'+k_2B')\right)d_{112}\theta$$
$$+\left(B_{22}^sk_2+B_{12}^sk_1\right)d_2\theta=0, \tag{20b}$$

$$B_{11}d_{111}u_0+(B_{12}+2B_{66})d_{122}u_0+(B_{12}+2B_{66})d_{112}v_0+B_{22}d_{222}v_0$$
$$-D_{11}d_{1111}w_0-2(D_{12}+2D_{66})d_{1122}w_0-D_{22}d_{2222}w_0$$
$$+\left(D_{11}^sk_1+D_{12}^sk_2\right)d_{11}\theta+2\left(D_{66}^s(k_1A'+k_2B')\right)d_{1122}\theta$$
$$+\left(D_{12}^sk_1+D_{22}^sk_2\right)d_{22}\theta+N_x^0d_{11}w_0+2N_{xy}^0d_{12}w_0+N_y^0d_{22}w_0=0 \tag{20c}$$

$$-\left(B_{11}^sk_1+B_{12}^sk_2\right)d_1u_0-\left(B_{66}^s(k_1A'+k_2B')\right)d_{122}u_0-\left(B_{66}^s(k_1A'+k_2B')\right)d_{112}v_0$$
$$-\left(B_{12}^sk_1+B_{22}^sk_2\right)d_2v_0+\left(D_{11}^sk_1+D_{12}^sk_2\right)d_{11}w_0+2\left(D_{66}^s(k_1A'+k_2B')\right)d_{1122}w_0$$
$$+\left(D_{12}^sk_1+D_{22}^sk_2\right)d_{22}w_0-H_{11}^sk_1^2\ \theta-H_{22}^s\ k_2^2\,\theta-2H_{12}^s\,k_1\,k_2\theta$$
$$-\left((k_1A'+k_2B')^2H_{66}^s\right)d_{1122}\theta+A_{44}^s(k_2B')^2d_{22}\theta+A_{55}^s\ (k_1\ A')^2\ d_{11}\theta=0 \tag{20d}$$

where d_{ij}, d_{ijl} and d_{ijlm} are the following differential operators:

$$d_{ijl}=\frac{\partial^3}{\partial x_i\partial x_j\partial x_l},\quad d_{ijl}=\frac{\partial^3}{\partial x_i\partial x_j\partial x_l},$$
$$d_{ijlm}=\frac{\partial^4}{\partial x_i\partial x_j\partial x_l\partial x_m},\quad (i,j,l,m=1,2). \tag{21}$$

The Navier solution method is employed to determine the analytical solutions for which the displacement variables are written as product of arbitrary parameters and known trigonometric functions to respect the equations of motion and boundary conditions.

$$\begin{Bmatrix}u_0\\ v_0\\ w_0\\ \theta\end{Bmatrix}=\sum_{m=1}^{\infty}\sum_{n=1}^{\infty}\begin{Bmatrix}U_{mn}\cos(\alpha x)\sin(\beta y)\\ V_{mn}\sin(\alpha x)\cos(\beta y)\\ W_{mn}\sin(\alpha x)\sin(\beta y)\\ X_{mn}\sin(\alpha x)\sin(\beta y)\end{Bmatrix} \tag{22}$$

With

$$\alpha=m\pi/a\quad\text{and}\quad\beta=n\pi/b \tag{23}$$

The plate is subjected to two types of loading, a transverse load q and in-plane forces in two directions

$N_x^0 = \gamma_1 N_{cr}$, $N_y^0 = \gamma_2 N_{cr}$, $N_{xy}^0 = 0$.

$$\begin{bmatrix} S_{11} & S_{12} & S_{13} & S_{14} \\ S_{12} & S_{22} & S_{23} & S_{24} \\ S_{13} & S_{23} & S_{33}+k & S_{34} \\ S_{14} & S_{24} & S_{34} & S_{44} \end{bmatrix} \begin{Bmatrix} U_{mn} \\ V_{mn} \\ W_{mn} \\ X_{mn} \end{Bmatrix} = \begin{Bmatrix} 0 \\ 0 \\ 0 \\ 0 \end{Bmatrix} \tag{24}$$

Where

$$\begin{aligned} S_{11} &= -\left(A_{11}\alpha^2 + A_{66}\beta^2\right), \quad S_{12} = -\alpha\beta\left(A_{12} + A_{66}\right), \\ S_{13} &= \alpha\left(B_{11}\alpha^2 + B_{12}\beta^2 + 2B_{66}\beta^2\right), \\ S_{14} &= \alpha\left(k_1 B_{11}^s + k_2 B_{12}^s - (k_1 A' + k_2 B')B_{66}^s\beta^2\right), \\ S_{22} &= -\left(A_{66}\alpha^2 + A_{22}\beta^2\right), \\ S_{23} &= \beta\left(B_{22}\beta^2 + B_{12}\alpha^2 + 2B_{66}\alpha^2\right), \\ S_{24} &= \beta\left(k_2 B_{22}^s + k_1 B_{12}^s - (k_1 A' + k_2 B')B_{66}^s\alpha^2\right) \\ S_{33} &= -\left(D_{11}\alpha^4 + 2(D_{12} + 2D_{66})\alpha^2\beta^2 + D_{22}\beta^4\right), \\ S_{34} &= -k_1\left(D_{11}^s\alpha^2 + D_{12}^s\beta^2\right) + 2(k_1 A' + k_2 B')\,D_{66}^s\alpha^2\beta^2 \\ &\quad - k_2\left(D_{22}^s\beta^2 + D_{12}^s\alpha^2\right), \\ S_{44} &= -k_1\left(H_{11}^s k_1 + H_{12}^s k_2\right) - (k_1 A' + k_2 B')^2 H_{66}^s\alpha^2\beta^2 \\ &\quad - k_2\left(H_{12}^s k_1 + H_{22}^s k_2\right) - (k_1 A')^2 A_{55}^s\alpha^2 - (k_2 B')^2 A_{44}^s\beta^2 \end{aligned} \tag{25}$$

Where

$$k = N_{cr}\left(\gamma_1\alpha^2 + \gamma_2\beta^2\right) \tag{26}$$

3. Numerical results

In this numerical study, effects of the porosity distributions, the porosity parameters, geometry parameters of plates and stacking sequence of layers on the critical buckling loads of the functionally graded sandwich simply-supported plates are investigated. The sandwich FGM plate is composed of Aluminum face sheets (as metal) and Alumina core (as ceramic). Young's modulus and Poisson's ratio of Aluminum are E_m=70 GPa, v_m=0.3 respectively, and those of Alumina are E_c=380 GPa, v_c=0.3. The following dimensionless form is used:

$$\overline{N} = \frac{N_{cr} a^2}{100 E_0 h^3} \tag{27}$$

Some kinds of symmetric and non-symmetric FGM sandwich plate are used as follows;

The (1-0-1) FGM sandwich plate: The plate is made of two layers of equal thickness withouta core:

$$h_1 = h_3 = h/2,\ h_2 = 0$$

The (1-1-1) FGM sandwich plate: The plate is made of three equal-thickness layers:

$$h_1 = h_2 = h_3 = h/3$$

The (1-2-1) FGM sandwich plate: The core thickness equals the sum of faces thickness:

$$h_1 = h_3 = h/4,\ h_2 = h/2$$

The (2-1-2) FGM sandwich plate: The upper layer thickness is twice the core layer while it is the same as the lower one:

$$h_1 = h_3 = 2h/5,\ h_2 = h/5$$

The (2-2-1) FGM sandwich plate: The core thickness is twice the upper face while it is the same as the lower one.

$$h_1 = h_2 = 2h/5,\ h_3 = h/5$$

In order to validate proposed model, a comparison study is performed. In the validation study, non-dimensional critical buckling load of square FGM sandwich plates with different stacking sequences andvolume fraction index *k* are presented and compared with the results obtained from this theory and those obtained by Zenkour (2005) based on sinusoidal shear deformation theory (SSDT), trigonometric shear deformation theory (TSDT), the first-order shear deformation theory (FSDT), a new hyperbolic shear deformation theory by El Meiche *et al.* 2011 and the new first-order shear deformation developed by Thai *et al.* (2014) for uniaxial and biaxial compressive loads in table 1 and table 2, respectively, for *a/h*=10.

It is seen from Tables 1 and 2, a good agreement between the results of the present theory with other theories. In the present theory includes only four unknowns in contrast with five unknowns in the SSDT, TSDT and FSDT. In addition, the using shear deformation theory does not require a shear correction factor as FSDT. So, the using shear deformation theory can be useful and more practice in the modelling of the composite plates.

In Fig. 3, the effect the side-to-thickness ratio *a/h* on the dimensionless critical buckling loads of (2-1-2) rectangular sandwich plates for *b*=2a, *n*=2 and *α*=0.2 with uniaxial and biaxial compression loads.

As seen from Fig. 3, the critical buckling loads increase with the increasing of the side-to-thickness ratio *a/h*, naturally. The critical buckling loads for uniaxial load are bigger than the critical buckling loads for biaxial load. The difference between the results of uniaxial and biaxial compression loads increase by increasing the ratio of *a/h*, significantly. The load type is very effective in the buckling responses of sandwich plates.

In Fig. 4, the effects of power law index *n* on the dimensionless critical buckling load $\overline{N}$ of square plates under biaxial compression are presented. As seen from fig. 4, the dimensionless critical buckling load decreases with increasing of the power law index because of Eq. (1) and selected materials. The increasing in the power law index

Table 1 Comparison of nondimensional critical buckling load of square FGM sandwich plates subjected to uniaxial compressive load γ_1=-1, γ_2=0, a/h=10)

k	Theory	Scheme				
		1-0-1	2-1-2	1-1-1	2-2-1	1-2-1
0	HSDT (El Meiche *et al* . 2011)	13.0055	13.0055	13.0055	13.0055	13.0055
	SSDT (Zenkour, 2005)	13.0061	13.0061	13.0061	13.0061	13.0061
	TSDT (Zenkour, 2005)	13.0050	13.0050	13.0050	13.0050	13.0050
	FSDT (Zenkour, 2005)	13.0045	13.0045	13.0045	13.0045	13.0045
	NFSDT (Thai, 2014)	13.0045	13.0045	13.0045	13.0045	13.0045
	Present	13.0055	13.0055	13.0055	13.0055	13.0055
0.5	HSDT (El Meiche *et al* . 2011)	7.3638	7.9405	8.4365	8.8103	9.2176
	SSDT (Zenkour, 2005)	7.3657	7.9420	8.4371	8.8104	9.2167
	TSDT (Zenkour, 2005)	7.3644	7.9408	8.4365	8.8100	9.2168
	FSDT (Zenkour, 2005)	7.3373	7.9132	8.4103	8.7867	9.1952
	NFSDT (Thai, 2014)	7.3634	7.9403	8.4361	8.8095	9.2162
	Present	7.3652	7.9415	8.4368	8.8333	9.2166
1	HSDT (El Meiche *et al* . 2011)	5.1663	5.8394	6.4645	6.9495	7.5072
	SSDT (Zenkour, 2005)	5.1685	5.8412	6.4654	6.9498	7.5063
	TSDT (Zenkour, 2005)	5.1671	5.8401	6.4647	6.9494	7.5066
	FSDT (Zenkour, 2005)	5.1424	5.8138	6.4389	6.9257	7.4837
	NFSDT (Thai, 2014)	5.1648	5.8387	6.4641	6.9485	7.5056
	Present	5.1680	5.8408	6.4652	7.0009	7.5063
5	HSDT (El Meiche *et al* . 2011)	2.6568	3.0414	3.5787	4.1116	4.7346
	SSDT (Zenkour, 2005)	2.6601	3.0441	3.5806	4.1129	4.7349
	TSDT (Zenkour, 2005)	2.6582	3.0426	3.5796	4.1121	4.7347
	FSDT (Zenkour, 2005)	2.6384	3.0225	3.5596	4.0929	4.7148
	NFSDT (Thai, 2014)	2.6415	3.0282	3.5710	4.1024	4.7305
	Present	2.6595	3.0436	3.5803	4.2339	4.7348
10	HSDT (El Meiche *et al* . 2011)	2.4857	2.7450	3.1937	3.7069	4.2796
	SSDT (Zenkour, 2005)	2.4893	2.7484	3.1946	3.1457	4.3818
	TSDT (Zenkour, 2005)	2.4873	2.7463	3.1947	3.7075	4.2799
	FSDT (Zenkour, 2005)	2.4690	2.7263	3.1752	3.6889	4.2604
	NFSDT (Thai, 2014)	2.4666	2.7223	3.1795	3.6901	4.2728
	Present	2.4887	2.7475	3.1956	3.8406	4.2802

Table 2 Comparison of nondimensional critical buckling load of square FGM sandwich plates subjected to biaxial compressive load (γ_1=-1, γ_2=0, a/h=10)

k	Theory	Scheme				
		1-0-1	2-1-2	1-1-1	2-2-1	1-2-1
0	HSDT (El Meiche *et al* . 2011)	6.5028	6.5028	6.5028	6.5028	6.5028
	SSDT (Zenkour, 2005)	6.5030	6.5030	6.5030	6.5030	6.5030
	TSDT (Zenkour, 2005)	6.5025	6.5025	6.5025	6.5025	6.5025
	FSDT (Zenkour, 2005)	6.5022	6.5022	6.5022	6.5022	6.5022
	NFSDT (Thai, 2014)	6.5022	6.5022	6.5022	6.5022	6.5022
	Present	6.5028	6.5028	6.5028	6.5028	6.5028
0.5	HSDT (El Meiche *et al* . 2011)	3.6819	3.9702	4.2182	4.4051	4.6088
	SSDT (Zenkour, 2005)	3.6828	3.9710	4.2186	4.4052	4.6084
	TSDT (Zenkour, 2005)	3.6822	3.9704	4.2182	4.4050	4.6084
	FSDT (Zenkour, 2005)	3.6687	3.9566	4.2052	4.3934	4.5976
	NFSDT (Thai, 2014)	3.6817	3.9702	4.2181	4.4047	4.6081
	Present	3.6826	3.9708	4.2184	4.4166	4.6083
1	HSDT (El Meiche *et al* . 2011)	2.5832	2.9197	3.2323	3.4748	3.7536
	SSDT (Zenkour, 2005)	2.5842	2.9206	3.2327	3.4749	3.7531
	TSDT (Zenkour, 2005)	2.5836	2.9200	3.2324	3.4747	3.7533
	FSDT (Zenkour, 2005)	2.5712	2.9069	3.2195	3.4629	3.7418
	NFSDT (Thai, 2014)	2.5824	2.9193	3.2320	3.4742	3.7528
	Present	2.5840	2.9204	3.2326	3.5004	3.7532
5	HSDT (El Meiche *et al* . 2011)	1.3284	1.5207	1.7894	2.0558	2.3673
	SSDT (Zenkour, 2005)	1.3300	1.5220	1.7903	2.0564	2.3674
	TSDT (Zenkour, 2005)	1.3291	1.5213	1.7898	2.0561	2.3673
	FSDT (Zenkour, 2005)	1.3192	1.5113	1.7798	2.0464	2.3574
	NFSDT (Thai, 2014)	1.3208	1.5141	1.7855	2.0512	2.3652
	Present	1.3298	1.5218	1.7902	2.1169	2.3674
10	HSDT (El Meiche *et al* . 2011)	1.2429	1.3725	1.5969	1.8534	2.1398
	SSDT (Zenkour, 2005)	1.2448	1.3742	1.5973	1.5729	2.1909
	TSDT (Zenkour, 2005)	1.2436	1.3732	1.5974	1.8538	2.1400
	FSDT (Zenkour, 2005)	1.2345	1.3631	1.5876	1.8445	2.1302
	NFSDT (Thai, 2014)	1.2333	1.3612	1.5897	1.8450	2.1364
	Present	1.2444	1.3738	1.5978	1.9203	2.1401

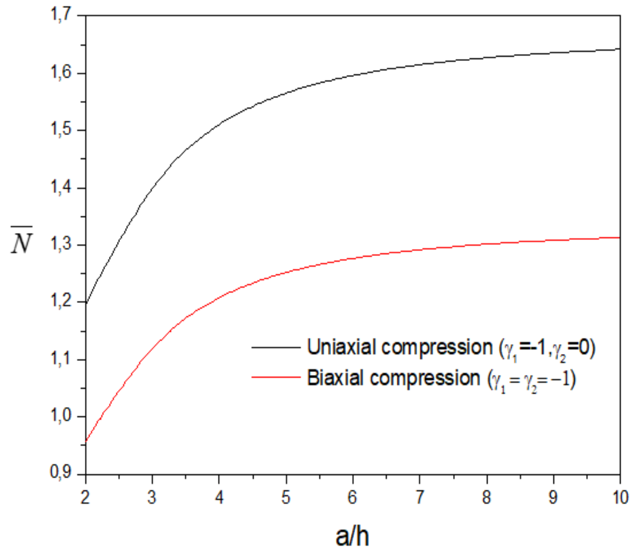

Fig. 3 Comparison of dimensionless critical buckling load $\overline{N}$ of (2-1-2) FGM sandwich rectangular plates (b=2a, n=2)

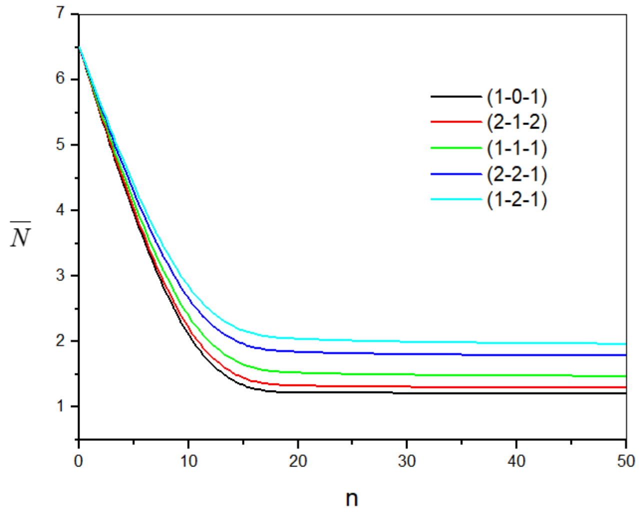

Fig. 4 Effect of power law index n on the dimensionless critical buckling load $\overline{N}$ of square plates under biaxial compression (γ_1=γ_2=-1, a=10h)

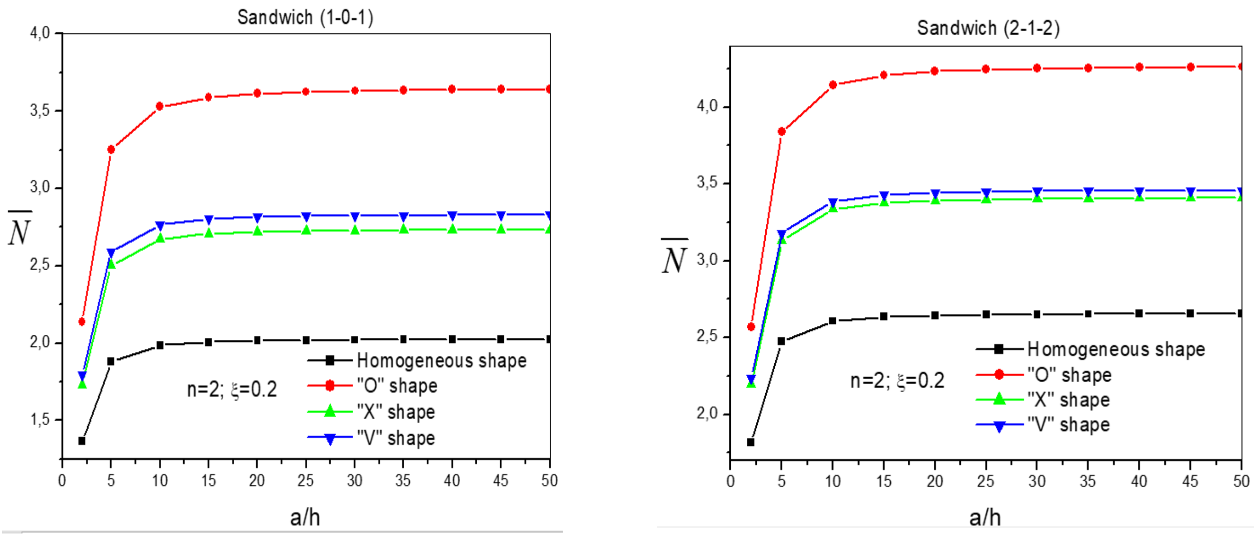

(a) for (1-0-1) scheme

(b) for (2-1-2) scheme

Fig. 5 Continued

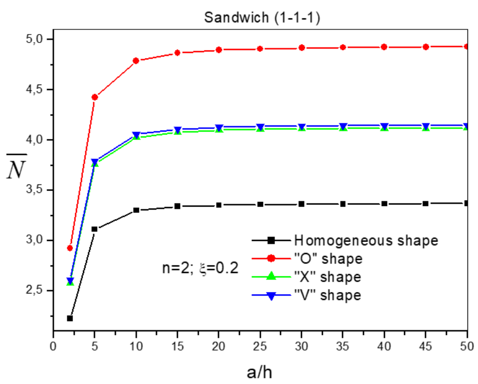

(c) for (1-1-1) scheme

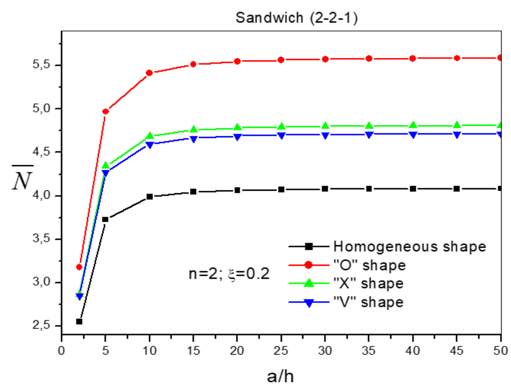

(d) for (2-2-1) scheme

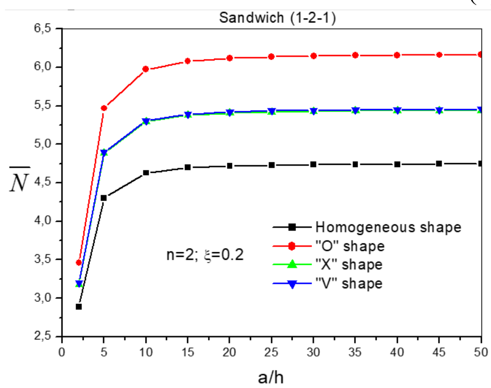

(e) for (1-2-1) scheme

Fig. 5 Effect of the shape of porosity distribution on the dimensionless critical buckling load $\overline{N}$ versus side-to-thickness a/h of an FGM square sandwich plate for different schemes under uniaxial compression ($\gamma 1=-1$, $\gamma 2=0$)

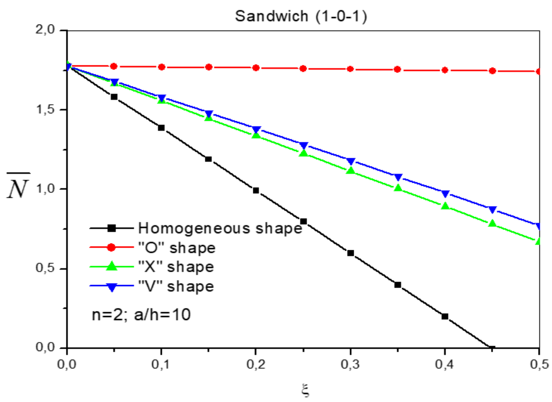

(a) for (1-0-1) scheme

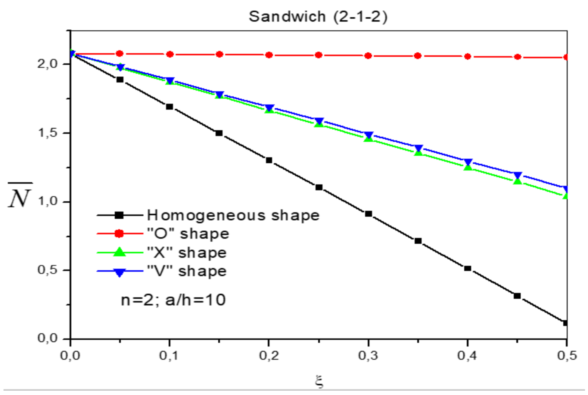

(b) for (2-1-2) scheme

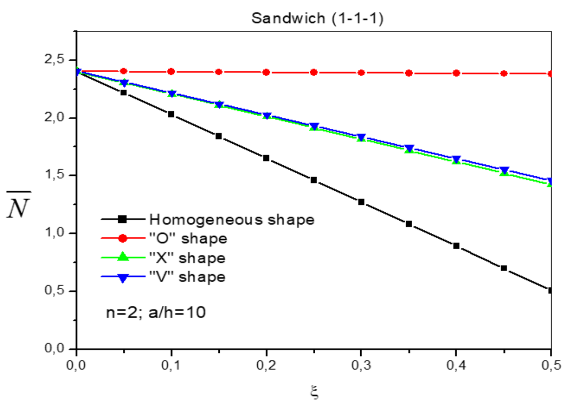

(c) for (1-1-1) scheme

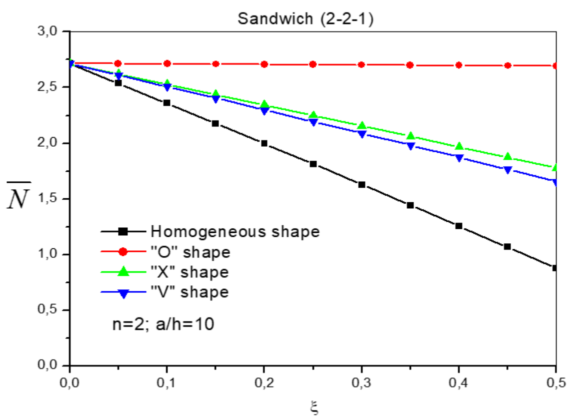

(d) for (2-2-1) scheme

Fig. 6 Continued

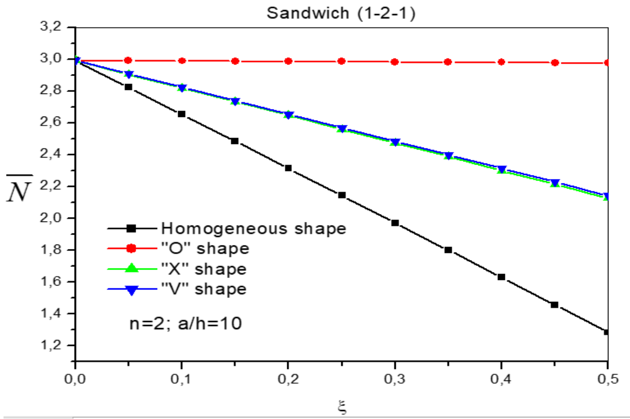

(e) for (1-2-1) scheme

Fig. 6 Effect of porosity coefficient on the dimensionless critical buckling load $\overline{N}$ of FGM sandwich plate for different schemes under biaxial compression (n=2)

yields to increase the difference among of the results in the stacking sequences. The biggest value of the dimensionless critical buckling load is obtained in the 1-2-1 scheme. The power law index has more effects on the buckling responses of sandwich FGM plates.

In Fig. 5, the relationship between side-to-thickness (a/h) and dimensionless critical buckling load under uniaxial compression is presented for different porosity models for different schemes of layers for n=2 and ξ=0.2. It is seen from Fig. 5 that the difference among the porosity models increases with increasing of a/h ratio. In higher values of a/h, the porosity distributions play important role on the buckling behavior of sandwich FGM porous plates. In all schemes of layers, the critical buckling loads of "O" porosity distribution are biggest values. The result of the homogeneous porosity model gives lowest values of critical buckling loads in all schemes. The reason of this situation is that the void more stack in the "homogeneous" porosity distribution, and so the rigidity of the plates is lowest in the "homogeneous" porosity model. As a result, "homogeneous" porosity model gives lowest the critical buckling loads in contrast with other porosity models.

Fig. 6 shows the effects of porosity coefficient (ξ) on the dimensionless critical buckling load under biaxial compression for different schemes of layers for n=2 and a/h=10. As seen from Fig. 6, increasing the porosity coefficient (ξ) yields to increase the difference among of porosity models, significantly. The results of "X" and "V" porosity models are very close to each other in (1-1-1) and (1-2-1) schemes. However, this difference is not close in (1-0-1), (2-1-2) and (2-1-2) schemes. It shows that the scheme of layer is very effective on the buckling and porosity behaviors sandwich FGM plates. With choosing of suitable layer scheme, the negative effects of porosity may be reduced.

4. Conclusions

In this study, buckling behavior of sandwich plates with porous FGM layers are investigated by using hyperbolic shear displacement model. Four type porosity models are used. In the solution of the problem, the Navier method is used. Effects of porosity coefficient, porosity models, FGM distribution parameter, side-to-thickness ratio, scheme of layers on the critical buckling loads of FGM sandwich plates are investigated for different compression load types. It is obtained from the numerical results the side-to-thickness ratio is very influences on the porosity effects for FGM sandwich plates. The buckling behavior of the FGM sandwich plates on the porosity effects change with different scheme of layers, significantly. Also, FGM distribution parameter has more effects on the effects of porosity on buckling responses. With changing of FGM distribution parameter and layer scheme, the negative effects of porosity can be reduced, considerably.

Briefly, the following results were obtained:

- The values of dimensionless critical buckling load of FG sandwich plate decrease with the increase of the power-law index.
- The type of porosity distribution model plays an important role in the behavior of FG porous sandwich plates, especially for high values of side to thickness ratio.
- In all lay-up schemes, the homogenous porosity model has the lowest the dimensionless critical buckling load.
- The difference between the porosity models increases with the increase of porosity volume fraction.

References

Abualnour, M., Chikh, A., Hebali, H., Kaci, A., Tounsi, A., Bousahla, A.A. and Tounsi, A. (2019), "Thermomechanical analysis of antisymmetric laminated reinforced composite plates using a new four variable trigonometric refined plate theory", *Comput. Concrete*, **24**(6), 489-498. https://doi.org/10.12989/cac.2019.24.6.489.

Addou, F.Y., Meradjah, M., Bousahla, A.A., Benachour, A., Bourada, F., Tounsi, A. and Mahmoud, S.R. (2019), "Influences of porosity on dynamic response of FG plates resting on Winkler/Pasternak/Kerr foundation using quasi 3D HSDT", *Comput. Concrete*, **24**(4), 347-367. https://doi.org/10.12989/cac.2019.24.4.347.

Alimirzaei, S., Mohammadimehr, M. and Tounsi, A. (2019), "Nonlinear analysis of viscoelastic micro-composite beam with geometrical imperfection using FEM: MSGT electro-magneto-elastic bending, buckling and vibration solutions", *Struct. Eng. Mech.*, **71**(5), 485-502. https://doi.org/10.12989/sem.2019.71.5.485.

Akbaş, Ş.D. (2017), "Vibration and static analysis of functionally graded porous plates", *J. Appl. Comput. Mec.*, **3**(3),199-207. https://doi.org/10.22055/JACM.2017.21540.1107.

Avcar, M. (2019), "Free vibration of imperfect sigmoid and power law functionally graded beams", *Steel and Composite Structures*, **30**(6), 603-615. https://doi.org/10.12989/scs.2019.30.6.603.

Asghar, S., Naeem, M.N., Hussain, M., Taj, M., and Tounsi, A. (2020), "Prediction and assessment of nonlocal natural frequencies of DWCNTs: Vibration analysis", *Comput. Concrete*, **25**(2), 133-144. https://doi.org/10.12989/cac.2020.25.2.133.

Balubaid, M., Chikh, A., Hebali, H., Kaci, A., Tounsi, A., Bousahla, A.A., and Tounsi, A. (2020), "Free vibration investigation of FG nanoscale plate using nonlocal two variables integral refined plate theory", *Comput. Concrete*, **24**(6), 579-586. https://doi.org/10.12989/cac.2019.24.6.579.

Batou, B., Nebab, M., Bennai, R., Ait Atmane, H., Tounsi, A. and Bouremana, M. (2019), "Wave dispersion properties in imperfect sigmoid plates using various HSDTs", *Steel Compos. Struct.*, **33**(5), 699- 716. https://doi.org/10.12989/scs.2019.33.5.699.

Belbachir, N., Draiche, K., Bousahla, A.A., Bourada, M., Tounsi, A. and Mohammadimehr, M. (2019), "Bending analysis of anti-symmetric cross-ply laminated plates under nonlinear thermal and mechanical loadings", *Steel Compos. Struct.*, **33**(1), 81-92. https://doi.org/10.12989/scs.2019.33.1.081.

Belbachir, N., Bourada, M., Draiche, K., Tounsi, A., Bourada, F., Bousahla, A.A. and Mahmoud, S.R. (2020), "Thermal flexural analysis of anti-symmetric cross-ply laminated plates using a four variable refined theory", *Smart Struct. Syst.*, **25**(4), 409-422. https://doi.org/10.12989/sss.2020.25.4.409.

Bellal, M., Hebali, H., Heireche, H., Bousahla, A.A., Tounsi, A., Bourada, F., Mahmoud, S.R., Adda Bedia, E.A. and Tounsi, A. (2020), "Buckling behavior of a single-layered graphene sheet resting on viscoelastic medium via nonlocal four-unknown integral model", *Steel Compos. Struct.*, **34**(5), 643-655. https://doi.org/10.12989/scs.2020.34.5.643.

Benahmed, A., Fahsi, B., Benzair, A., Zidour, M., Bourada, F. and Tounsi, A. (2019), "Critical buckling of functionally graded nanoscale beam with porosities using nonlocal higher-order shear deformation", *Struct. Eng. Mech.*, **69**(4), 457-466. https://doi.org/10.12989/sem.2019.69.4.457.

Bennai, R., Fourn, H., Ait Atmane, H., Tounsi, A. and Bessaim, A. (2019), "Dynamic and wave propagation investigation of FGM plates with porosities using a four variable plate theory", *Wind Struct.*, **28**(1), 49-62. https://doi.org/10.12989/was.2019.28.1.049.

Berghouti, H., Adda Bedia, E.A., Benkhedda, A. and Tounsi, A. (2019), "Vibration analysis of nonlocal porous nanobeams made of functionally graded material", *Advan. Nano Res.*, **7**(5), 351-364. https://doi.org/10.12989/anr.2019.7.5.351.

Bourada, F., Bousahla, A.A., Bourada, M., Azzaz, A., Zinata, A. and Tounsi, A. (2019), "Dynamic investigation of porous functionally graded beam using a sinusoidal shear deformation theory", *Wind Struct.*, **28**(1), 19-30. https://doi.org/10.12989/was.2019.28.1.019.

Bourada, F., Bousahla, A.A., Tounsi, A., Adda Bedia, E.A., Mahmoud, S.R., Benrahou, K.H. and Tounsi, A. (2020), "Stability and dynamic analyses of SW-CNT reinforced concrete beam resting on elastic-foundation", *Comput. Concrete*, **25**(6), 485-495. http://doi.org/10.12989/cac.2020.25.6.485.

Bousahla, A.A., Bourada, F., Mahmoud, S.R., Tounsi, A., Algarni, A., Adda Bedia, E.A. and Tounsi, A. (2020a), "Buckling and dynamic behavior of the simply supported CNT-RC beams using an integral-first shear deformation theory", *Comput. Concrete*, **25**(2), 155-166. https://doi.org/10.12989/cac.2020.25.2.155.

Boussoula, A., Boucham, B., Bourada, M., Bourada, F., Tounsi, A., Bousahla, A.A. and Tounsi, A. (2020b), "A simple nth-order shear deformation theory for thermomechanical bending analysis of different configurations of FG sandwich plates", *Smart Struct. Syst.*, **25**(2), 197-218. https://doi.org/10.12989/sss.2020.25.2.197.

Boutaleb, S., Benrahou, K.H., Bakora, A., Algarni, A. Bousahla, A.A., Tounsi, A., Tounsi, A. and Mahmoud, S.R. (2019), "Dynamic Analysis of nanosize FG rectangular plates based on simple nonlocal quasi 3D HSDT", *Advan. Nano Res.*, **7**(3), 191-208. https://doi.org/10.12989/anr.2019.7.3.191.

Chikr, S.C., Kaci, A., Bousahla, A.A., Bourada, F., Tounsi, A., Adda Bedia, E.A., Mahmoud, S.R., Benrahou, K.H. and Tounsi, A. (2020), "A novel four-unknown integral model for buckling response of FG sandwich plates resting on elastic foundations under various boundary conditions using Galerkin's approach", *Geomech. Eng.*, **21**(5), 471-487. https://doi.org/10.12989/gae.2020.21.5.471.

Draiche, K., Bousahla, A.A., Tounsi, A., Alwabli, A.S., Tounsi, A. and Mahmoud, S.R. (2019), "Static analysis of laminated reinforced composite plates using a simple first-order shear deformation theory", *Comput. Concrete*, **24**(4), 369-378. https://doi.org/10.12989/cac.2019.24.4.369.

Ebrahimi, F. and Jafari, A. (2016), "A higher-order thermomechanical vibration analysis of temperature-dependent FGM beams with porosities", *J. Eng.* http://doi.org/10.1155/2016/9561504.

El Meiche, N., Tounsi, A., Ziane, N. andMechab, I. (2011), "A new hyperbolic shear deformation theory for buckling and vibration of functionally graded sandwich plate", *Int. J. Mech. Sci.*, **53**(4), 237-247. https://doi.org/10.1016/j.ijmecsci.2011.01.004.

Fazzolari, F.A. (2018), "Generalized exponential, polynomial and trigonometric theories for vibration and stability analysis of porous FG sandwich beams resting on elastic foundations", *Compos. Part B: Eng.*, **136**, 254-271. https://doi.org/10.1016/j.compositesb.2017.10.022.

Hadji, L., Zouatnia, N. and Bernard, F. (2019), "An analytical solution for bending and free vibration responses of functionally graded beams with porosities: Effect of the micromechanical models", *Struct. Eng. Mech.*, **69**(2), 231-241. https://doi.org/10.12989/sem.2019.69.2.231.

Hadji, L. and Avcar, M. (2021), "Free vbration analysis of FG porous sandwich plates under various boundary conditions", *J. Appl. Comput. Mech.*, https://doi.org/10.22055/JACM.2020.35328.2628.

Hussain, M., Naeem, M.N., Tounsi, A. and Taj, M. (2019), "Nonlocal effect on the vibration of armchair and zigzag SWCNTs with bending rigidity", *Advan. Nano Res.*, **7**(6), 431-442. https://doi.org/10.12989/anr.2019.7.6.431.

Hussain, M., Nawaz Naeem, M., Shabaz Khan, M. and Tounsi, A. (2020a), "Computer-aided approach for modelling of FG cylindrical shell sandwich with ring supports", *Comput. Concrete*, **25**(5), 411-425. https://doi.org/10.12989/cac.2020.25.5.411.

Hussain, M., Nawaz Naeem, M., Taj, M. and Tounsi, A. (2020b), "Simulating vibration of single-walled carbon nanotube using

Rayleigh-Ritz's method", *Advan. Nano Res.*, **8**(3), 215-228. https://doi.org/10.12989/anr.2020.8.3.215.

Jouneghani, F.Z., Dimitri, R. and Tornabene, F. (2018), "Structural response of porous FG nanobeams under hygro-thermo-mechanical loadings", *Composites Part B: Eng .*, **152**, 71-78. https://doi.org/10.1016/j.compositesb.2018.06.023.

Kaddari, M., Kaci, A., Bousahla, A.A., Tounsi, A., Bourada, F., Tounsi, A., Adda Bedia, E.A. and Al-Osta, M.A. (2020), "A study on the structural behaviour of functionally graded porous plates on elastic foundation using a new quasi-3D model: Bending and free vibration analysis", Comput. Concrete, **25**(1), 37-57. https://doi.org/10.12989/cac.2020.25.1.037.

Karamanli, A. and Aydogdu, M. (2020), "Bifurcation buckling conditions of FGM plates with different boundaries", *Compos. Struct.*, **245**, 112325. https://doi.org/10.1016/j.compstruct.2020.112325.

Karami, B., Janghorban, M. and Tounsi, A. (2019), "Galerkin's approach for buckling analysis of functionally graded anisotropic nanoplates/different boundary conditions", *Eng. Comput.*, **35**, 1297-1316. https://doi.org/10.1007/s00366-018-0664-9.

Keddouri, A., Hadji, L. and Tounsi, A. (2019), "Static analysis of functionally graded sandwich plates with porosities", *Advan. Mater. Res.*, **8**(3), 155-177. https://doi.org/10.12989/amr.2019.8.3.155.

Matouk, H., Bousahla, A.A., Heireche, H., Bourada, F., Adda Bedia, E.A., Tounsi, A. and Benrahou, K.H. (2020), "Investigation on hygro-thermal vibration of P-FG and symmetric S-FG nanobeam using integral Timoshenko beam theory", *Advan. Nano Res.*, **8**(4), 293-305. https://doi.org/10.12989/anr.2020.8.4.293.

Medani, M., Benahmed, A., Zidour, M., Heireche, H., Tounsi, A., Bousahla, A.A., Tounsi, A. and Mahmoud, S.R. (2019), "Static and dynamic behavior of (FG-CNT) reinforced porous sandwich plate using energy principle", *Steel Compos. Struct.*, **32**(5), 595-610. https://doi.org/10.12989/scs.2019.32.5.595.

Rahmani, M.C., Kaci, A., Bousahla, A.A., Bourada, F., Tounsi, A., Adda Bedia, E.A., Mahmoud, S.R., Benrahou, K.H. and Tounsi, A. (2020), "Influence of boundary conditions on the bending and free vibration behavior of FGM sandwich plates using a four-unknown refined integral plate theory", *Comput. Concrete*, **25**(3), 225-244. https://doi.org/10.12989/cac.2020.25.3.225.

Ramteke, P.M., Panda, S.K. and Sharma, N. (2019), "Effect of grading pattern and porosity on the eigen characteristics of porous functionally graded structure", *Steel Compos. Struct.*, **33**(6), 865. https://doi.org/10.12989/scs.2019.33.6.865.

Refrafi, S., Bousahla, A.A., Bouhadra, A., Menasria, A., Bourada, F., Tounsi, A., Adda Bedia, E.A., Mahmoud, S.R., Benrahou, K.H. and Tounsi, A. (2020), "Effects of hygro-thermo-mechanical conditions on the buckling of FG sandwich plates resting on elastic foundations", *Comput. Concrete*, **25**(4), 311-325. https://doi.org/10.12989/cac.2020.25.4.311.

Safa, A., Hadji, L., Bourada, M. and Zouatnia, N. (2019), "Thermal vibration analysis of FGM beams Using an efficient shear deformation beam theory", *Earthq. Struct.*, **17**(3), 329-336. https://doi.org/10.12989/eas.2019.17.3.329.

Sahla, M., Saidi, H., Draiche, K., Bousahla, A.A. Bourada, F. and Tounsi, A. (2019), "Free vibration analysis of angle-ply laminated composite and soft core sandwich plates", "*Steel Compos. Struct.*, **33**(5), 663-679. https://doi.org/10.12989/scs.2019.33.5.663.

Shariati, A., Ghabussi, A., Habibi, M., Safarpour, H., Safarpour, M., Tounsi, A. and Safa, M. (2020a), "Extremely large oscillation and nonlinear frequency of a multi-scale hybrid disk resting on nonlinear elastic foundations", *Thin-Walled Struct.*, **154**, 106840. https://doi.org/10.1016/j.tws.2020.106840.

Shariati, A., Habibi, M., Tounsi, A., Safarpour, H. and Safa, M. (2020b), "Application of exact continuum size-dependent theory for stability and frequency analysis of a curved cantilevered microtubule by considering viscoelastic properties", *Eng. Comput.*, https://doi.org/10.1007/s00366-020-01024-9.

Taati, E. and Fallah, F. (2019), "Exact solution for frequency response of sandwich microbeams with functionally graded cores", *J. Vib. Control*, **25**(19-20), 2641-2655. https://doi.org/10.1177/1077546319864645.

Taj, M., Majeed, A., Hussain, M., Naeem, M.N., Safeer, M., Ahmad, M., Ullah Khan, H. and Tounsi, A. (2020), "Non-local orthotropic elastic shell model for vibration analysis of protein microtubules", *Comput. Concrete*, **25**(3), 245-253. https://doi.org/10.12989/cac.2020.25.3.245.

Thai, H.T., Nguyen, T.K., Vo, T.P. and Lee, J. (2014), "Analysis of functionally graded sandwich plates using a new first-order shear deformation theory", *Europ. J. Mech.-A/Solids*, **45**, 211-225. https://doi.org/10.1016/j.euromechsol.2013.12.008.

Tounsi, A., Al-Dulaijan, S.U., Al-Osta, M.A., Chikh, A., Al-Zahrani, M.M., Sharif, A. and Tounsi, A. (2020), "A four variable trigonometric integral plate theory for hygro-thermo-mechanical bending analysis of AFG ceramic-metal plates resting on a two-parameter elastic foundation", *Steel Compos. Struct.*, **34**(4), 511-524. https://doi.org/10.12989/scs.2020.34.4.511.

Trinh, L.C., Vo, T.P., Thai, H.T., Nguyen, T.K. and Keerthan, P. (2018), "State-space Levy solution for size-dependent static, free vibration and buckling behaviours of functionally graded sandwich plates", *Composs Part B*, **149**, 144-164, https://doi.org/10.1016/j.compositesb.2018.05.017.

Wattanasakulpong, N. and Ungbhakorn, V. (2014), "Linear and nonlinear vibration analysis of elastically restrained ends FGM beams with porosities", *Aerosp. Sci. Technol.*, **32**(1), 111-120. https://doi.org/10.1016/j.ast.2013.12.002.

Wu, D., Liu, A., Huang, Y., Huang, Y., Pi, Y. and Gao, W. (2018), "Dynamic analysis of functionally graded porous structures through finite element analysis", *Eng. Struct.*, **165**, 287-301. https://doi.org/10.1016/j.engstruct.2018.03.023.

Xu, K., Yuan, Y. and Li, M. (2019), "Buckling behavior of functionally graded porous plates integrated with laminated composite faces sheets", *Steel Compos. Struct.*, **32**(5), 633-642. https://doi.org/10.12989/scs.2019.32.5.633.

Yang, J., Chen, D. and Kitipornchai, S. (2018), "Buckling and free vibration analyses of functionally graded graphene reinforced porous nanocomposite plates based on Chebyshev-Ritz method", *Compos. Struct.*, **193**, 281-294. https://doi.org/10.1016/j.compstruct.2018.03.090.

Zhao, J., Xie, F., Wang, A., Shuai, C., Tang, J. and Wang, Q. (2019), "Vibration behavior of the functionally graded porous (FGP) doubly-curved panels and shells of revolution by using a semi-analytical method", *Compos. Part B: Engineering*, **157**, 219-238. https://doi.org/10.1016/j.compositesb.2018.08.087.

Zenkour, A.M. (2005), "A comprehensive analysis of functionally graded sandwich plates: Part 1-Deflection and stresses", *Int. J. Solids Struct.*, **42**(18-19), 5224-5242. https://doi.org/10.1016/j.ijsolstr.2005.02.015.

Zenkour, A.M., Sobhy, M. (2010), "Thermal buckling of various types of FGM sandwich plates", *Compos. Struct.*, **93**(1), 93-102. https://doi.org/10.1016/j.compstruct.2010.06.012

Zhu, J., Lai, Z., Yin, Z., Jeon, J. and Lee, S. (2001), "Fabrication of ZrO_2–NiCr functionally graded material by powder metallurgy", *Mater. Chem. Phys*, **68**, 130-135. https://doi.org/10.1016/j.prostr.2020.06.006.

CC